ISSN 1807-1929
Revista Brasileira de Engenharia Agrícola e Ambiental
Brazilian Journal of Agricultural and Environmental Engineering
v.25, n.1, p.58-64, 2021
Campina Grande, PB – http://www.agriambi.com.br – http://www.scielo.br/rbeaa

DOI: http://dx.doi.org/10.1590/1807-1929/agriambi.v25n1p58-64

Numerical-experimental comparison of radial fans applied in pneumatic transport of agricultural fertilizer spreaders[1]

Comparação numérico-experimental de ventiladores radiais aplicados em transporte pneumático de adubadores agrícolas

Marcelo L. de F. Fogal[2*], Gustavo B. Micheli[2], Vicente L. Scalon[2] & Alcides Padilha[2]

[1] Research developed at Universidade Estadual Paulista "Julio de Mesquita Filho", Faculdade de Engenharia de Bauru, Departamento de Engenharia Mecânica, Bauru, SP, Brasil
[2] Universidade Estadual Paulista "Julio de Mesquita Filho"/Faculdade de Engenharia de Bauru/Departamento de Engenharia Mecânica, Bauru, SP, Brasil

HIGHLIGHTS:

The methodology used represents the numerical simulation of radial fans properly.
The mesh, convergence and turbulence parameters are significant in the numerical-experimental comparison.
The numerical results, analysed by CFX software, were similar to the experimental results.

ABSTRACT: This study presents a numerical and experimental comparison of two different types of radial fans used in an agricultural fertilizer spreader at a rotation of 4000 rpm. The numerical analysis was validated through experiments conducted on a test bench using a hot-wire anemometer for velocity measurements and a Pitot tube for pressure readings. A simulation of the agricultural fertilizer spreader was carried out after the experimental validation of the mathematical models of the radial fans on the test bench to evaluate the air distribution behavior along the application nozzles, which was compared to the experimental results. A turbulent mean-field was obtained using the Reynolds Averaged Navier Stokes (RANS) and the k-Epsilon turbulence model was used for two equations. The computational fluid dynamics software CFX 18.1 was used to solve the transport equations. Unstructured tetrahedral meshes generated by the ICEM CFD 18.1 software were used in all models. The applied method is adequate and able to reproduce the fluid-dynamic behavior of airflow in pneumatic systems of agricultural fertilizer spreaders, avoiding the need for prototypes.

Key words: turbulence model, computational fluid dynamics, CFX, hot-wire anemometer, Pitot tube

RESUMO: Este estudo apresenta um comparativo numérico-experimental de dois tipos de rotores radiais utilizados em um sistema de adubação agrícola a uma rotação de 4000 rpm. Para validação da análise numérica realizaram-se experimentos em uma bancada de testes utilizando um anemômetro de fio quente para as medidas de velocidade e um tubo de Pitot para as tomadas de pressão. Após a validação experimental dos modelos matemáticos dos rotores em bancada foi realizada uma simulação do sistema de aplicação do adubador agrícola para avaliar o comportamento da distribuição de ar ao longo dos bocais de aplicação e comparado aos resultados experimentais. O campo médio turbulento foi obtido com a média de Reynolds (Reynolds Averaged Navier Stokes – RANS) e o modelo de turbulência utilizado para o fechamento do conjunto de equações foi o modelo k-Épsilon. O software da dinâmica computacional do fluido CFX 18.1 foi utilizado para a obtenção das soluções das equações de transporte. Em todos os modelos foram utilizadas malhas não estruturadas tetraédricas geradas pelo software ICEM CFD 18.1. Verificou-se que a metodologia empregada é adequada e apta a reproduzir o comportamento fluidodinâmico do escoamento de ar em sistemas de transporte pneumático de adubadores agrícolas, evitando a necessidade de protótipos.

Palavras-chave: modelo de turbulência, fluidodinâmica computacional, CFX, anemômetro de fio quente, tubo de Pitot

• Ref. 225923 – Received 11 Jul, 2019
* Corresponding author - E-mail: marcelo.fogal@hotmail.com
• Accepted 09 Oct, 2020 • Published 18 Nov, 2020
Edited by: Walter Esfrain Pereira

Introduction

The growing increase in the world population has led to the need to produce more and in a smaller area, and good agricultural productivity requires that nutrients be in an adequate amount for plants (Camargo, 2012). Some machines that perform the agricultural fertilization use the airflow to transport fertilizers to the application nozzles, providing uniform and precise distribution.

These machines need a fan coupled to the system to generate the flow, creating an energy gradient that allows the desired airflow. Companies have invested in studies to optimize the fertilization systems aiming at improving the application quality. For this, experimental tests or mathematical modeling can be performed using numerical methods.

Computational fluid dynamics (CFD) allows obtaining numerical solutions for problems with complex geometries and imposed boundary conditions. The CFD techniques for turbomachinery modeling are the best tool for understanding certain complex aerodynamic phenomena characteristic of this type of flow. Studies developed by Junaidi et al. (2015), Lam & Peng (2016), and Zhang & Baar (2018) showed that this technique is widely applied to various types of turbomachinery.

Several numerical/experimental studies have investigated the development and characteristics of the airflow. Vibhakar (2012) studied the flow behavior of a radial fan with backward- and forward-curved blades using CFD techniques and the software Gambit and Fluent by ANSYS and found data similar to those of the experimental results. The simulations validated the project method, showing parameters of fan performance and regions of high recirculation that were improved with changes in geometry.

Fan optimization using the finite volumes method has been successfully used for several years, replacing traditional project methods that require prototyping and instrumentation. The finite volumes method is extensively described in the literature, and its application was discussed by Jeong & Seong (2014), Yang & Jiang (2010), and Lorenzi et al. (2016).

This study aimed to evaluate the behavior of two types of radial fans applied to an agricultural fertilization system and the velocity distribution in the application nozzles of an agricultural fertilizer spreader through numerical simulation compared to the results obtained experimentally.

Material and Methods

The mathematical model used in this study is based on the Navier-Stokes equations, considering the three-dimensional flow, steady-state, and compressible fluid with ideal gas behavior, but disregarding the influence of the gravitational field and turbulent flow. A turbulent mean-field was obtained with the Reynolds Averaged Navier Stokes (RANS) and the k-Epsilon turbulence model.

The computational fluid dynamics software CFX 18.1 was used to obtain the solution of the transport equations, with the finite volumes as the numerical method. Unstructured tetrahedral meshes generated by the ICEM CFD 18.1 software were used in all models.

The governing equations are integrated to allow the relevant quantity (e.g., mass, movement, and energy) to be conserved for each control volume. The equations solved for the discretized flow domain are equations of conservation of mass (Eq. 1), momentum (Eq. 2), and energy (Eq. 3). Turbulent viscosity (μ_t) is determined through additional terms that were solved using the turbulence model of two k-Epsilon equations (Eqs. 4 and 5):

$$\frac{\partial \rho}{\partial t} + \frac{\partial}{\partial x_j}\left(\rho U_j\right) = 0 \quad (1)$$

$$\frac{\partial}{\partial t}\left(\rho U_i\right) + \frac{\partial}{\partial x_j}\left(\rho U_i U_j\right) = -\frac{\partial P}{\partial x_i} - \frac{\partial \tau_{ij}}{\partial x_j} + \rho f_i \quad (2)$$

$$\frac{\partial}{\partial t}\left(\rho H\right) + \frac{\partial}{\partial x_j}\left(\rho U_j H\right) = \frac{\partial P}{\partial t} - \frac{\partial}{\partial x_j}\left(U_i \tau_{ij} + q_j\right) + \rho U_i f_i \quad (3)$$

$$\frac{\partial\left(\rho k\right)}{\partial t} + \frac{\partial\left(\rho U_j k\right)}{\partial x_j} = \frac{\partial}{\partial x_j}\left(\left(\mu + \frac{\mu_t}{\sigma_k}\right)\frac{\partial k}{\partial x_j}\right) + P_k - \rho\varepsilon \quad (4)$$

$$\frac{\partial\left(\rho\varepsilon\right)}{\partial t} + \frac{\partial\left(\rho U_j \varepsilon\right)}{\partial x_j} = \frac{\partial}{\partial x_j}\left(\left(\mu + \frac{\mu_t}{\sigma_\varepsilon}\right)\frac{\partial \varepsilon}{\partial x_j}\right) + \frac{\varepsilon}{k}\left(C_{\varepsilon 1} P_k - \rho C_{\varepsilon 2}\varepsilon\right) \quad (5)$$

where:

ρ - fluid specific mass, kg m^{-3};

t - time, s;

U_i and U_j - velocity vectors, m s^{-1};

P - static pressure, Pa;

τ_{ij} - viscous tensor, Pa s;

f_i - field forces, N;

H - total enthalpy, J;

q_j - energy transferred, J;

μ - dynamic viscosity of the fluid, Pa s;

μ_t - turbulent viscosity, Pa s;

k - turbulent kinetic energy, m^2 s^{-2};

ε - dissipation rate of the turbulent kinetic energy, m^2 s^{-3};

P_k - production of turbulence due to viscous forces, Pa s^{-1}; and,

$C_{\varepsilon 1}$, $C_{\varepsilon 2}$, σ_k, and σ_ε - empirical constants with values of 1.44; 1.92; 1.0 and 1.3 respectively (Ansys CFX reference guide, 2013).

The meshes were generated using the ANSYS ICEM 18.1 software because of the complexity of the rotating domain geometries. This software allows more control to create the mesh and has tools to improve its quality. The mesh used in all models was an unstructured tetrahedral mesh, which is easier to refine in regions of geometric complexity.

The time step option was the local timescale factor, which has a different time step for each volume control until it reaches the pre-established convergence criterion (residuals between interactions lower than 10^{-4}).

The test bench models of the air distribution system with radial fans A1 and B1 are composed of three subdomains: a

rotating subdomain representing the radial fan (1) and two downstream stationary subdomains representing the volute (2) and the air distribution box (3), as shown in Figures 1 and 2.

A periodicity interface was used to reduce the number of elements and processing time, representing the rotational domain reduced to the blade angle. The interface between subdomains 1 and 2 is the fluid-fluid type with an angle variation, while the interface between subdomains 2 and 3 is the fluid-fluid type with an automatic connection. Fogal et al. (2014) used the same connection types for axial rotors, resulting in values closer to the experimental ones.

The model parameters in the pre-processing are defined as inlet at A with a zero relative total pressure and a temperature of 26.2 °C (experimental temperature), outlet at B with a zero relative static pressure, radial fan rotation at 4000 rpm, and smooth wall conditions and no slipping on the other surfaces.

This model with an A1 radial fan represents the complete agricultural fertilizer spreader system. It consists of four subdomains: a rotating subdomain with an A1 radial fan reduced to the blade angle (1) and three stationary subdomains with the volute (2), the air distribution box (3) and the pipes (4), as shown in Figure 3.

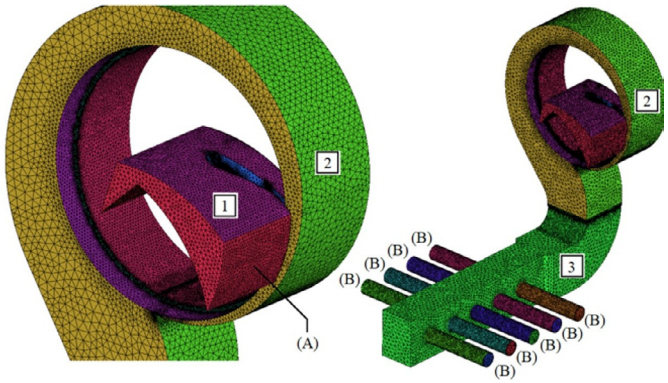

A - Inlet; B - Outlet; 1 - Fan; 2 - Volute; 3 - Air distribution box

Figure 1. Domain of the air distribution system with an A1 radial fan

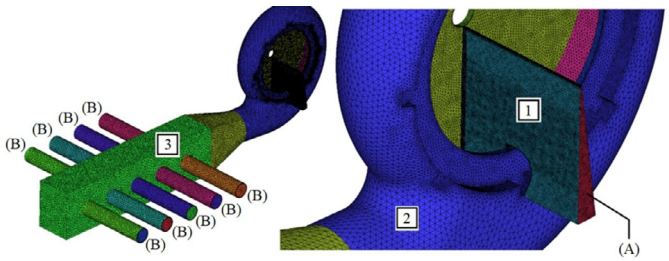

A - Inlet; B - Outlet; 1 - Fan; 2 - Volute; 3 - Air distribution box

Figure 2. Domain of the air distribution system with a B1 radial fan

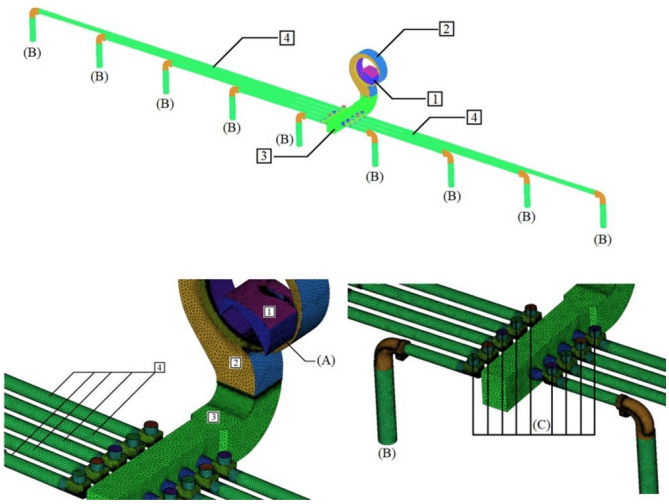

A - Inlet; B - Outlet; C - Opening; 1 - Fan; 2 - Volute; 3 - Air distribution box; 4 - Tubes

Figure 3. Application system of the agricultural fertilizer spreader

The model parameters are defined as inlet at A with zero relative total pressure and temperature of 33 °C (experimental temperature), outlet at B with zero relative static pressure, opening at C with zero relative static pressure and temperature of 33 °C, radial fan rotation at 4500 rpm, and smooth wall conditions and no slipping on the other surfaces.

The regions of the boundary condition at C are the inlets of solid particulate (fertilizer), which are not represented in this study. The particulate was assumed to follow the flow without interfering with its behavior.

Two test benches were used to validate the numerical models, representing the air distribution system of the agricultural fertilizer spreader, with the A1 (500 mm in diameter and 95 mm in width, with 12 blades) and B1 (330 mm in diameter and 65 mm in width, with 44 blades) fans coupled (Figures 4 and 5) using a Pitot tube for pressure measurements.

The tests resulted in quantitative values of pressure, flow, temperature, and power in the outlets of the nine nozzles at a rotation of 4000 rpm, which were compared to the numerical results.

The experiment on the complete system of the agricultural fertilizer spreader was carried out after validating the numerical models in the test bench (Figure 6). Velocity measurements were performed using a hot-wire anemometry at the nine application nozzles at a rotation of 4500 rpm (operation regime of the agricultural fertilizer spreader), and the velocities obtained numerically were compared.

Measurements of the ambient temperature and barometric pressure were carried out before all experiments to adjust the pressures. The measurements of the experimental results

Figure 4. Test bench with an A1 radial fan

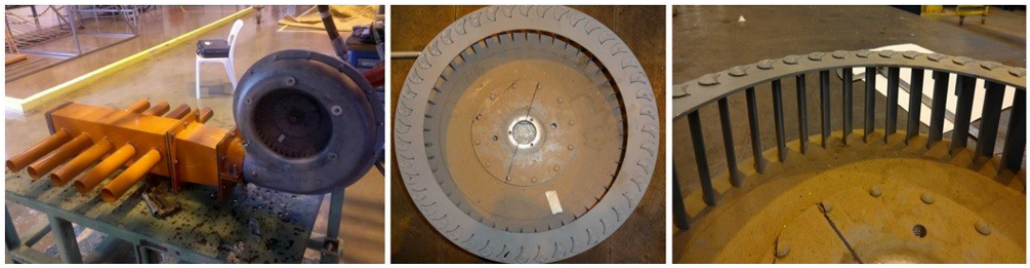

Figure 5. Test bench with a B1 radial fan

Figure 6. Agricultural fertilizer spreader

followed the standard for testing fans in the laboratory (ANSI/AMCA, 1999).

Results and Discussion

The results of the numerical and experimental comparison of the air distribution system in the test bench with A1 and B1 radial fans need to be evaluated for the values of the dimensionless Yplus (dimensionless distance relative to the wall and used as information on the mesh resolution) throughout the air distribution system to ensure that the results close to the wall are valid. In this study, Yplus must be lower than 300 for the k-Epsilon model (Micheli et al., 2015).

The highest values of Yplus considering the A1 radial fan model were observed in the reduction area region of the air distribution box, while the highest values in the B1 radial fan model occurred in a small area of the tip of the blade, with values lower than the maximum limit in both cases. Thus, the mesh is sufficiently refined for the adopted turbulence model.

Figures 7 and 8 show the velocity gradients in the central plane of the air distribution system, considering the lateral and top views in the test bench with A1 and B1 radial fans. The upper-velocity limit was set at 80 m s^{-1} to improve the view.

Figure 9 shows the streamlines in the air distribution system and the volute with A1 and B1 radial fans.

The numerical results in Figures 7 to 9 show that the air distribution system with the A1 radial fan has few regions with recirculations and uniform velocity distribution at the outlets compared to the system with the B1 radial fan. Figures 10 and 11 show the details of these recirculations in the models with A1 and B1 radial fans, respectively.

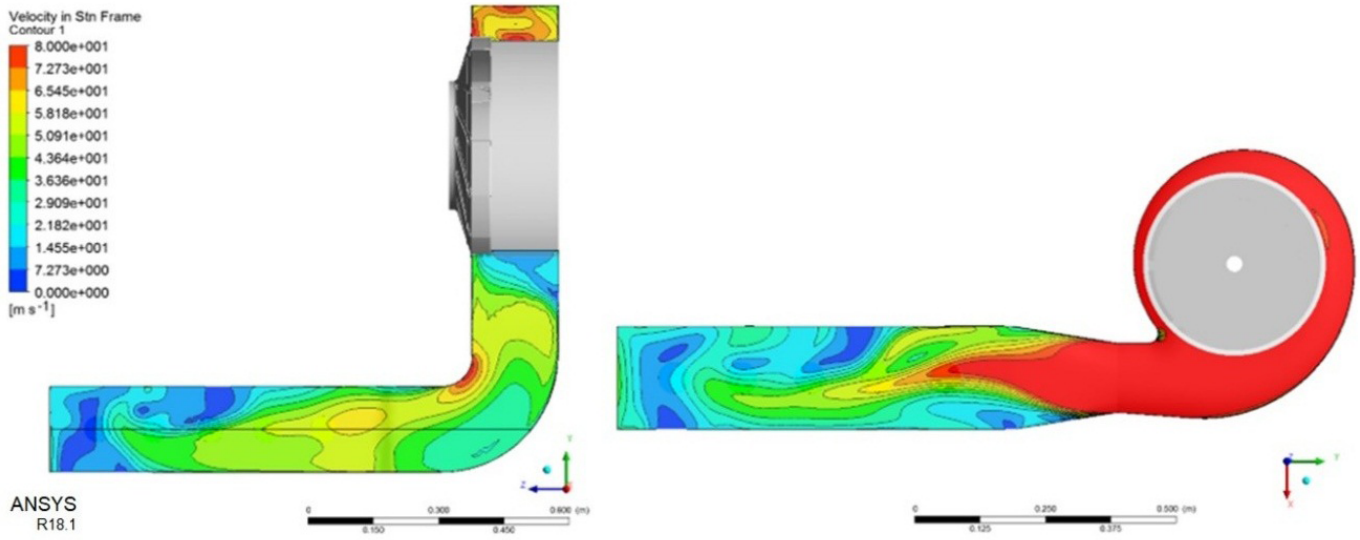

Figure 7. Velocity gradient in the central plane with the lateral view in the A1 and B1 radial fans

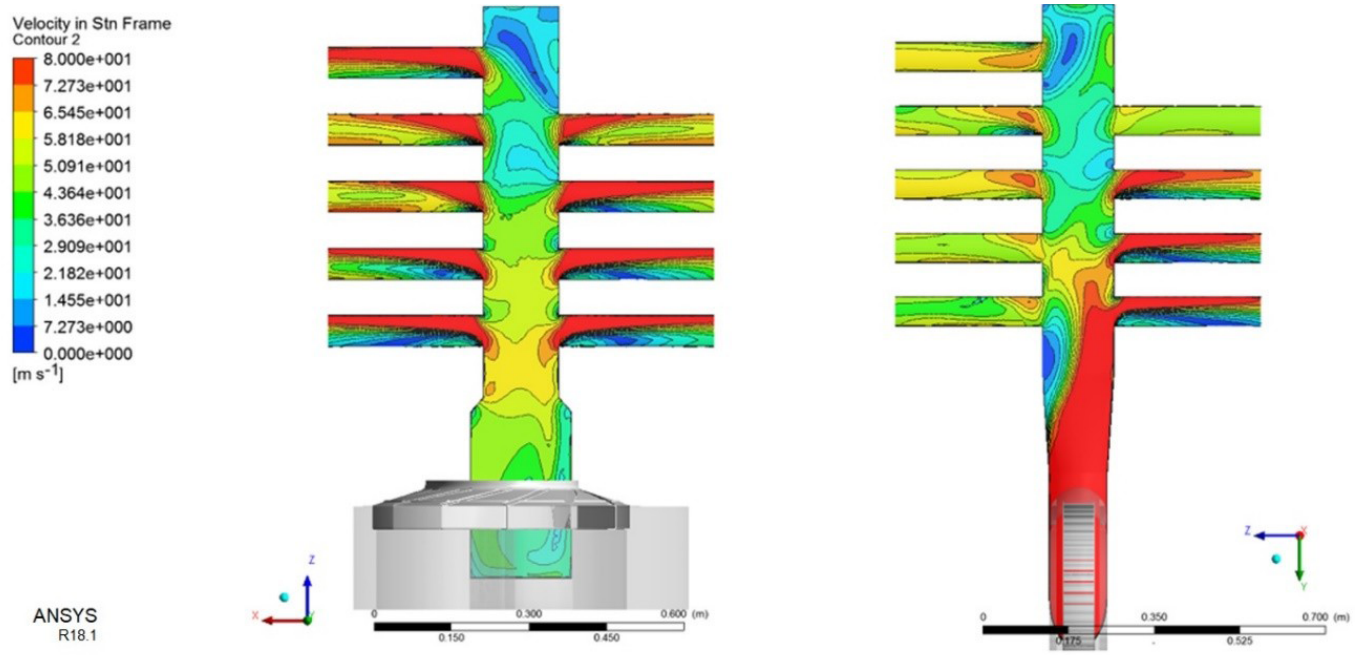

Figure 8. Velocity gradient in the central plane with the top view in the A1 and B1 radial fans

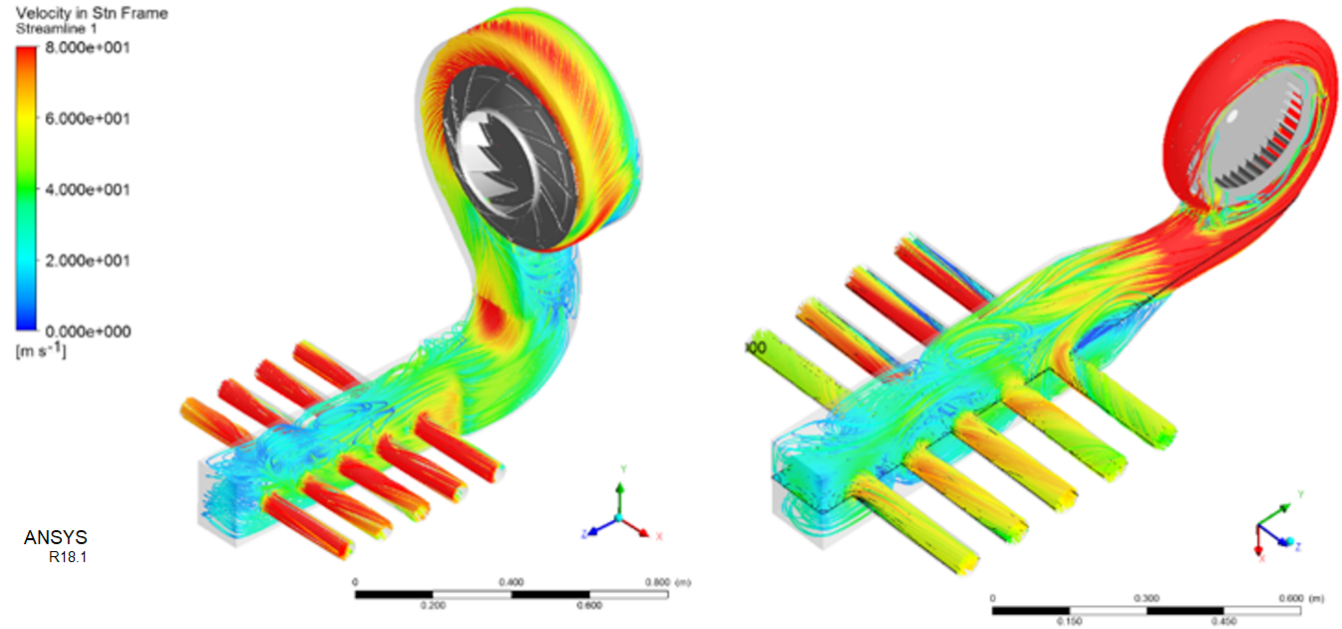

Figure 9. Streamlines in the A1 and B1 radial fans

Recirculations in the air distribution system with the A1 radial fan are concentrated in the final region of the air distribution box. However, the recirculations in the model with the B1 radial fan are in the entire box. Recirculations, especially in turbulent flows, as discussed here, promote a loss of energy from the fluid, which decreases the efficiency of the system.

Velocity values in the volute of the B1 radial fan were higher than in the volute of the A1 radial fan, which causes an increase of the head loss. Perhaps using the B1 radial fan in another application with lower rotation (reducing the head loss) and an air distribution box with a diameter similar to that of the volute results in a better flow behavior (with lower recirculation and better distribution), contributing to increasing the efficiency of the system. Table 1 shows a comparison between numerical and experimental results.

The numerical results followed the same trend of the experimental results. The efficiency of the system with the A1 radial fan is numerically 70% higher than the efficiency value of the system with the B1 radial fan.

The consumed power (9.2%) and efficiency (5.2%) were the variables that presented the highest difference between the numerical and experimental results regarding the A1 and B1 radial fans. This difference may be related to the mesh refinement, the convergence criterion (residual between iterations lower than 10^{-4}), the adopted turbulence model, or the experimental uncertainties.

The average difference between the variables of A1 and B1 radial fans was around 4.5 and 2.5%, respectively. It shows that the results are adequate for this type of analysis because a mesh refinement or a change in the convergence criterion and turbulence model would increase the computational cost.

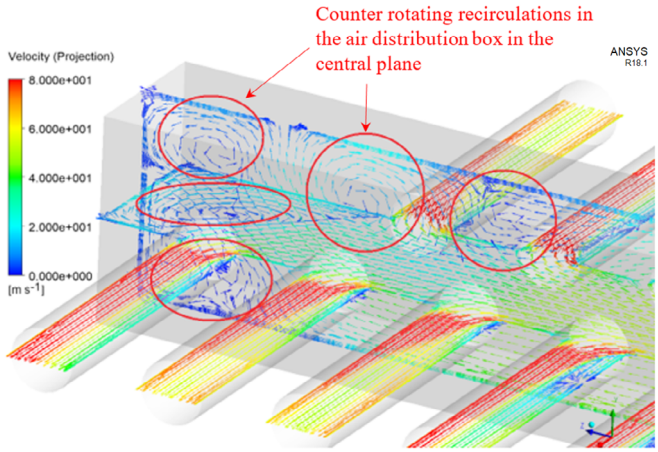

Figure 10. Detail of the recirculation in the air distribution box with the A1 radial fan

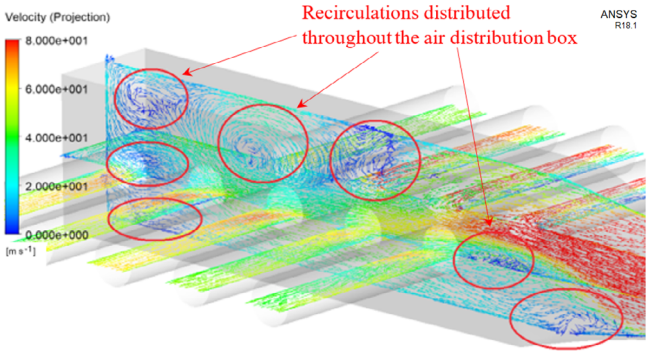

Figure 11. Detail of the recirculation in the air distribution box with the B1 radial fan

Figure 12 shows the velocity gradients in the central plane of the air distribution system in the top view and the numbered outlets in the pipes for the velocity evaluation.

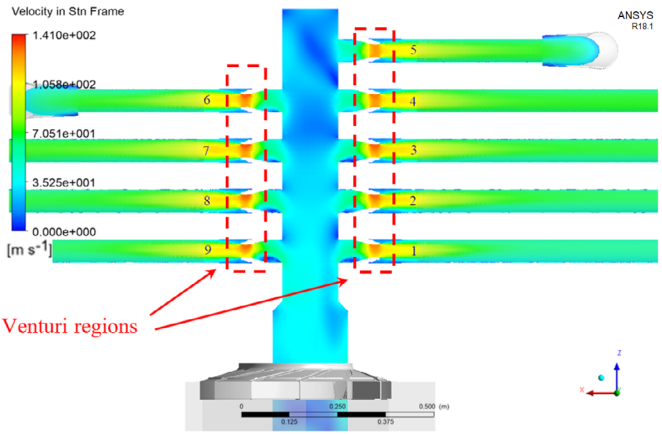

Figure 12. Detail of the velocity gradient in the central plane with the top view of the application system of the agricultural fertilizer spreader

The Venturi regions show an increase of velocity due to the constricted section. The velocity exceeds Mach 0.3 at some points, which is justified when considering the effect of air compressibility and the use of the perfect gas model.

Figure 13 shows the streamlines from the radial fan and the streamlines representing the airflow in the inlet regions of the solid particulate.

The highest recirculations were concentrated in the final part of the air distribution box, as already evaluated in the test bench model (Figure 10).

The flow gain relative to the flow imposed by the rotor due to the use of Venturis is 49.6% (region of the particle aspiration). Velocities at the outlets varied according to the pipe length due to the head loss. Figure 14 shows the velocity distribution comparison between the numerical results and those obtained experimentally.

Table 1. Comparison between numerical and experimental results

	A1 radial fan			B1 radial fan		
	Experimental	Numerical	Difference [%]	Experimental	Numerical	Difference [%]
Efficiency [%]	31.2	31.1	0.3	19.1	18.2	5.2
Flow [10^{-1} m^3 s^{-1}]	17.3	16.0	8.1	13.2	12.8	3.4
Power In [kW]	13.9	12.7	9.2	11.6	11.7	0.5
Temperature [°C]	34.7	33.4	3.8	35.2	34.4	2.2
Pressure [10^2 Pa]	25.1	24.7	1.3	16.7	16.5	1.1

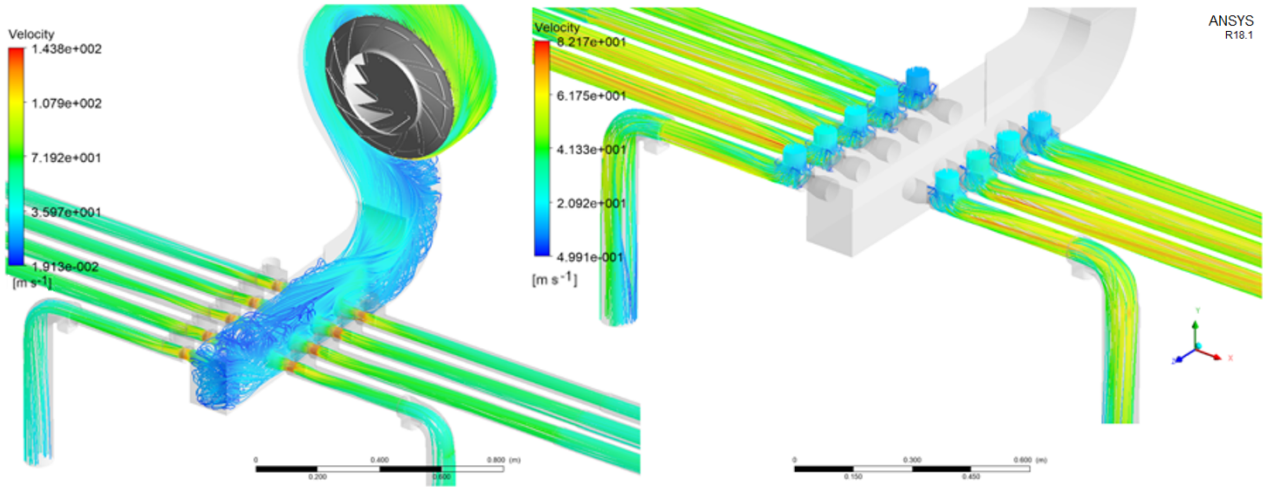

Figure 13. Streamlines in the application system of the agricultural fertilizer spreader

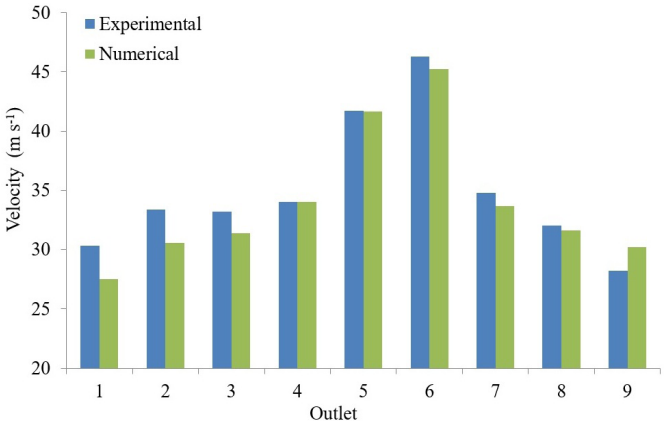

Figure 14. Numerical and experimental values of velocity at the outlets of the agricultural fertilizer spreader

The average difference between the numerical and experimental results were 4.3%, and the highest difference was around 10% at the outlet 1. These differences may be related to the mesh refinement, convergence criterion, turbulence model, and experimental uncertainties, as previously analyzed. The highest differences are associated with the tube length, and the use of a turbulence model that has a different treatment near the walls (such as the shear stress transport-SST) could result in values similar to the experimental result. However, this type of model requires more mesh refinement to attend the criteria of the wall (Yplus ≤ 2) and, consequently, a higher computational resource.

The standard deviations of velocities at the outlets of the application system were 5.8 and 5.7 m s^{-1} in the numerical and experimental analyses, respectively. Because the fertilizer dose is controlled and evenly distributed throughout the pipes, the airflow must ensure the particulate transport so that no clogging occurs. The velocity at the outlets must be higher than 25 m s^{-1} to meet the transported volume requirements. Figure 14 shows that the velocities are higher than this value at all outlets.

The adopted numerical model is considered adequate to represent the complete phenomenon of this application system because the result trends are the same and the differences are small.

Conclusions

1. The A1 radial fan was 70% more efficient in the test bench than the system with the B1 radial fan.

2. The average difference between the numerical and experimental results was 4.3% in the application system model of the agricultural fertilizer spreader. The highest differences were associated with the tube length.

3. The numerical results followed the same trends as the experimental results, and the main differences between these results may be related to the mesh refinement, convergence criterion, turbulence model, and experimental uncertainties.

4. The CFX software presented very reliable results and the method is adequate and able to reproduce the fluid-dynamic behavior of airflow in pneumatic systems of agricultural fertilizer spreaders without the need to create prototypes.

Literature Cited

ANSI/AMCA - An American National Standard. Laboratory Methods of Testing Fans for Aerodynamic Performance Rating. Arlington Heights: ANSI/AMCA, 1999. 69p.

Ansys CFX reference guide. Canonsburg, PA: Ansys Inc., 2013. 402p.

Camargo, M. S. A importância do uso de fertilizantes para o meio ambiente. Pesquisa & Tecnologia, v.9, p.1-3, 2012.

Fogal, M. L. F.; Padilha, A.; Scalon, V. L. Theoretical and experimental study of agricultural spraying using CFD. Journal of the Brazilian Society of Mechanical Sciences, v.36, p.125-138, 2014. https://doi.org/10.1007/s40430-013-0062-6

Jeong, W.; Seong, J. Comparison of effects on technical variances of computational fluid dynamics (CFD) software based on finite element and finite volume methods. International Journal of Mechanical Sciences, v.78, p.19-26, 2014. https://doi.org/10.1016/j.ijmecsci.2013.10.017

Junaidi, A. R.; Kumari, N. B. V. L.; Samad, M. A.; Ahmed, G. M. S. CFD simulation to enhance the efficiency of centrifugal pump by application of inner guide vanes. Materials Today Proceeding, v.2, p.2073-2082, 2015. https://doi.org/10.1016/j.matpr.2015.07.200

Lam, H.F.; Peng, H. Y. Study of wake characteristics of a vertical axis wind turbine by two- and three-dimensional computational fluid dynamics simulations. International Journal of Renewable Energy, v.90, p.386-398, 2016. https://doi.org/10.1016/j.renene.2016.01.011

Lorenzi, S.; Cammi, A.; Luzzi, L.; Rozza, G. POD-Galerkin method for finite volume approximation of Navier-Stokes and RANS equations. Computer Methods in Applied Mechanics and Engineering, v.311, p.151-179, 2016. https://doi.org/10.1016/j.cma.2016.08.006

Micheli, G. B.; Padilha, A.; Scalon, V. L. Numerical and experimental analysis of pesticide spray mixing in sprayer tanks. Journal of the Brazilian Association of Agricultural Engineering, v.35, p.1065-1078, 2015. http://dx.doi.org/10.1590/1809-4430-Eng.Agric.v35n6p1065-1078/2015

Vibhakar, N. N. Studies on radial tipped centrifugal fan. Surat: Veer Narmad South Gujarat University, 2012. 350p. Doctoral thesis

Yang, H.; Jiang, L. A dual mesh approach to enhance accuracy of the boundary conditions for unstructured grid modelling of turbomachinery flows. Asme Turbo EXPO, v.7, p.933-942, 2010. https://doi.org/10.1115/GT2010-23390

Zhang, F.; Baar, R. 3D-CFD-Study of Aerodynamic Losses in Compressor Impellers. SAE International Journal of Commercial Vehicles, v.11, p.191-200, 2018. https://doi.org/10.4271/02-11-03-0015